Self-Assembled Nanolayers of Conjugated Silane with π−π Interlocking

Jinyue Jiang,[†] Ocelio V. Lima,[†] Yong Pei,[‡] Zhang Jiang,[§] Ziguang Chen,[†] Chichao Yu,[†] Jin Wang,[§] Xiao Cheng Zeng,[‡] Eric Forsythe,[⊥] and Li Tan[†,*]

[†]Department of Engineering Mechanics and Nebraska Center for Materials and Nanoscience, University of Nebraska, Lincoln, Nebraska 68588, [‡]Department of Chemistry, University of Nebraska, Lincoln, Nebraska 68588, [§]Advanced Photon Source, Argonne National Laboratory, 9700 S. Cass Avenue, Argonne, Illinois 60439, and [⊥]Flexible Display Center, Army Research Laboratory, 2800 Powder Mill Road, Adelphi, Maryland 20783

ABSTRACT The packing of electronic molecules into planar structures and an ensured π−π interaction within the plane are preferred for efficient organic transistors. Thin films of organic electronics are exemplar, but the widely adopted molecular design and associated fabrication lead to limited ordering in multistack construction motifs. Here we demonstrate self-assembled nanolayers of organic molecules having potential electronic utility using an amphiphilic silane as a building block. Unlike a cross-linked (tetrahedral) configuration found in conventional siloxane networks, a linear polymer chain is produced following silane polycondensation. As a result, hydrophobic branches plus a noncovalent π−π interlocking between the molecules promote planar packing and continuous stacking along the surface normal. In contrast to conventional π−π stacking or hydrogen bonding pathways in a fibrous construct, multistacked nanolayers with coexisting π−π and herringbone interlocking can provide unmatched properties and processing convenience in molecular electronics.

KEYWORDS: self-assembly · nanolayer · π−π interlocking · conjugation · silane

Highly ordered, freestanding semiconducting layers with a unit thickness as small as a few nanometers are currently receiving wide attention from physical science researchers[1−3] researchers and are actively being investigated by the organic electronics[4−7] and sensor communities.[2,8−10] The surface-directed growth of monolayers has reached a level of maturity where many functional molecules, such as alkane thiols[11−14] or π-conjugates,[15−18] can be regulated by a S−Au bond or electrostatic interactions. While multistack construction using monolayers is possible, the widely practiced fabrication method of using a hydroxylated surface[19−21] limits ordering in the upper layers.

Freestanding and ordered structures can be constructed by using substrate-free pathways, achieved most commonly in a liquid environment through π−π stacking[22] or hydrogen bonding.[6,23,24] For example, organic electronic molecules can be designed to have π-units surrounded by alkyl chains. A one-dimensional (1D) structure can be assembled as a result of the π−π stacking between isolated π-units over the interruption caused by the van der Waals interaction from the alkyl groups.[22] Alternatively, H-bonding groups can be appended to organic electronic molecules to guide the formation of an ordered structure, and polypeptides or proteins with one or more β-sheet strands are natural candidates. When conjugated moieties are placed between these peptides, long, fibril nanostructures are produced.[6,23] Even though π−π stacking and hydrogen bonding can successfully produce freestanding 1D structures, grouping them further to produce a sheetlike object is less common due to the complexity in creating strong interactions or growth mechanisms in organic molecules in two different directions.

While it is difficult to pack many organic molecules into a freestanding object due to their weak intermolecular forces,[22] a layered stacking of organosilane (formula of $R-SiX_3$, R is alkyl and X can be halogen or alkoxy) is feasible and has captured the attention of the self-assembly community.[19,25−28] Unlike surface growth over silicon oxides, the driving forces for assembling these molecules together as amorphous lamellar structures is their coupled solvophobic and solvophilic interactions, as well as the subsequent occurring polycondensation.[25,27] Solvophobic interaction minimizes the exposure of siloxane tails (SiX_3) to solvents by stacking alkyl groups (R) toward the outer surfaces of nuclei. When cross-linking between the reactive tails occurs, construction of monolayers and a continuous stacking along the surface

*Address correspondence to ltan4@unl.edu.

Received for review February 9, 2010 and accepted May 26, 2010.

Published online June 2, 2010.
10.1021/nn100273m

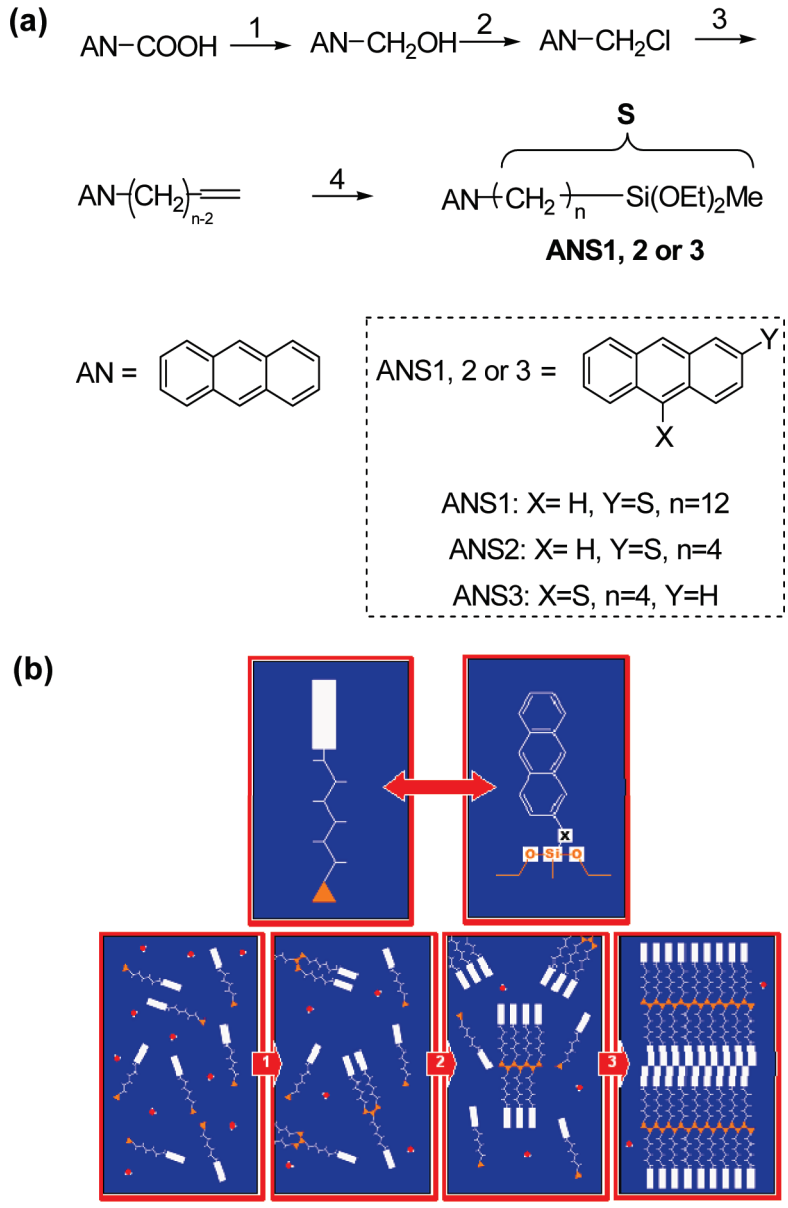

Scheme 1. (a) General synthetic route for ANS1-3 (inset: chemical structure). Conditions: (1) BH_3, THF, 50 °C, 6 h; (2) MsCl, CH_2Cl_2, r.t., overnight; (3) bromoalkene, magnesium, THF, 50 °C, 3 h; (4) diethoxymethylsilane, PtO_2, 24 h, 80 °C. (b) Side view illustration of the ANS1 self-assembly. (Step 1) Rigid heads interact through solvophobic and π−π interactions to preform well-organized nuclei; (step 2) hydrolysis and further condensation lead to the formation of polymers, from which a molecular layer can be formed *via* strong interaction between neighboring π units; and (step 3) multistacked nanolayers result from the repetition of the above processes

normal completes the lamellar stacking. There have been attempts to provide organosilanes with electronic functions by replacing the alkyl moiety with a bulky π-conjugated unit.[5,29,30] The resulting substrate-free assembly, however, revealed tubular structures rather than the expected planar objects. This was due, very likely, to the cross-linked (tetrahedral) configuration of the siloxane inside the two-dimensional (2D) network, where close packing or an ordered grouping of π-units in plane became unstable.[21,31,32] Presumably, when this very strained packing is partially relaxed by releasing the siloxane network to spatially aligned polysiloxane chains, a freestanding and highly ordered 2D object from the conjugated silane molecules may still be possible, and that is the focus of this paper.

To demonstrate our concept of planar construction, anthracene, a simple acene with three fused benzene rings, was used to represent the conjugated moiety on organosilane, and only two active terminals were stitched on a silicon atom. This design led to the building block, namely (12-(anthracen-2-yl)dodecyl)diethoxy(methyl)silane (henceforth referred to as ANS1, Scheme 1), for our nanostructure. The synthesis started with the reduction of 9,10-dioxo-9,10-dihydroanthracene-2-carboxylic acid by zinc under basic conditions, generating anthracene-2-carboxylic acid

(Scheme 1a). This acid was converted to alcohol, followed by chlorination. Coupling of the resulting 2-(chloromethyl)anthracene with the Grignard reagent, prepared from 11-bromoundec-1-ene, resulted in 2-(dodec-11-enyl)anthracene. The final hydrosilylation was performed in a sealed pressure tube and catalyzed by PtO_2. In all, ANS1 was produced in five steps with an overall yield of 15%. The reaction and characterization of the corresponding products can be found in the Methods section.

RESULTS AND DISCUSSION

By chemically bonding a rigid aromatic head with an alkylsilane tail, ANS1 appears to adopt a planar packing. We found layered nanostructures or nanolayers of ANS1 on substrates after the solution was drop-cast from tetrahydrofuran (THF). Atomic force microscopy (AFM) in Figure 1a reveals the flat terraces of such a structure, stacked over an area of *ca.* 50 × 50 μm^2. Figure 1b shows a histogram of four layers stacked vertically (inset in Figure 1a), indicating a layer height of 4.1 nm. Interestingly, these nanolayers can be peeled off from silicon wafers after an extended sonication. Figure 1c is a transmission electron microscopic (TEM) image of one of the flexible pieces with multiple layers held together. The inset in the same figure shows the stacking contrast of more than 20 layers.

X-ray diffraction (XRD) and grazing-incidence X-ray diffraction (GIXD) were used to further probe the excellent in- and out-of-plane orderings. Multiple sharp XRD peaks were observed (Figure 2a) with the strongest (001) measuring 39.96 Å; other higher-order peaks were noted from (002) to (008). This *d*-spacing represented the individual lamellar thickness along the *z*-direction, consistent with AFM measurements. The narrow width of the diffraction peak further suggested a *z*-directional ordering of *ca.* 112 nm, equivalent to a continuous stacking of 28 molecular layers. The relative electron density profile was plotted by using diffraction peaks from the first to the fifth orders and is depicted in the inset of Figure 2a, suggesting a periodic stacking of alternating organic and inorganic moieties. Moreover, the GIXD measurements in Figure 2b,c provide us with the in-plane lattice parameters, where a distorted centered rectangular unit cell with a coexisting $\pi-\pi$ and herringbone packing motif arranged in dimensions of $a_1 = 6.1$ Å, $a_2 = 8.1$ Å, and $\gamma = 88.8°$, can be assigned.

Snapshots of the growth process can be captured by using AFM imaging at the different stages of self-assembly. First, a silicon wafer was immersed in ANS1 solution. The molecules were allowed to adsorb onto the surfaces, followed by rinsing with pristine solvents. The surface was immediately found to be covered with a self-assembled monolayer. Above the monolayer, were multistacks of bilayer. As shown in Figure 3, ANS1

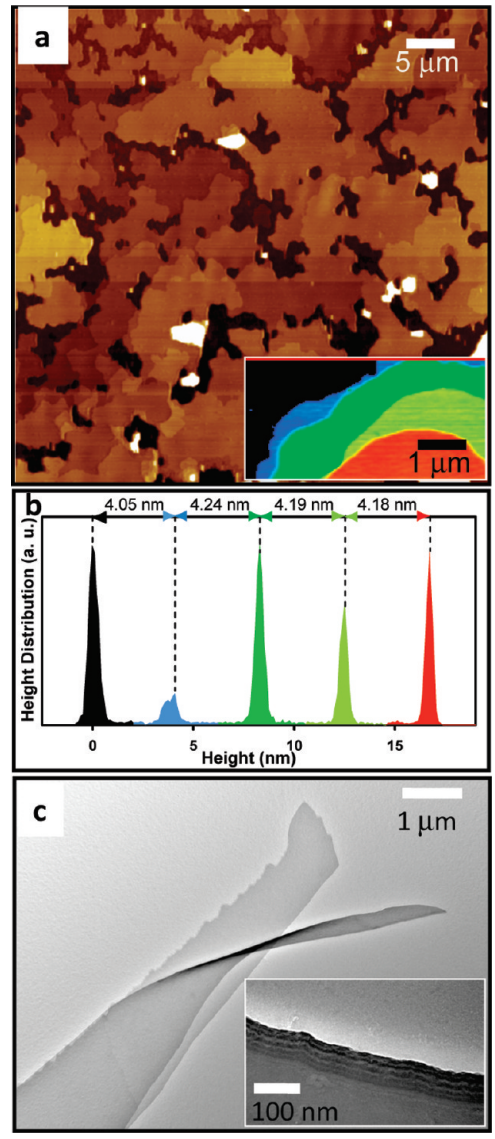

Figure 1. (a) AFM snapshot of the nanolayers covering an area of *ca.* 50 × 50 μm^2; (b) height distribution of continuously stacked four nanolayers (inset of panel a). Peak distance indicates an average layer height labeled at the top; and (c) freestanding, flexible nanolayers revealed by TEM. Inset shows edges of more than 20 continuous layers.

started to form a monolayer 2.4 nm in height after 5 min, which was consistent with how organosilane molecules usually orient themselves—almost vertically on the surface.[33] In 40 min, the monolayer had grown into a large, continuous film that covered almost the entire surface. In the meantime, only patches of bilayers at 4.3 nm in height were detected atop the monolayer. These patches slowly grew into stacks after 24 h; and by this time, the monolayer could no longer be seen. However, 2.4-nm-depth flaws were occasionally found inside the bilayer stacks, suggesting that a monolayer lay underneath. We found that the structure and morphology of assembled ANS1 are independent of the ANS1 concentration in THF, while the assembly rate increases with a

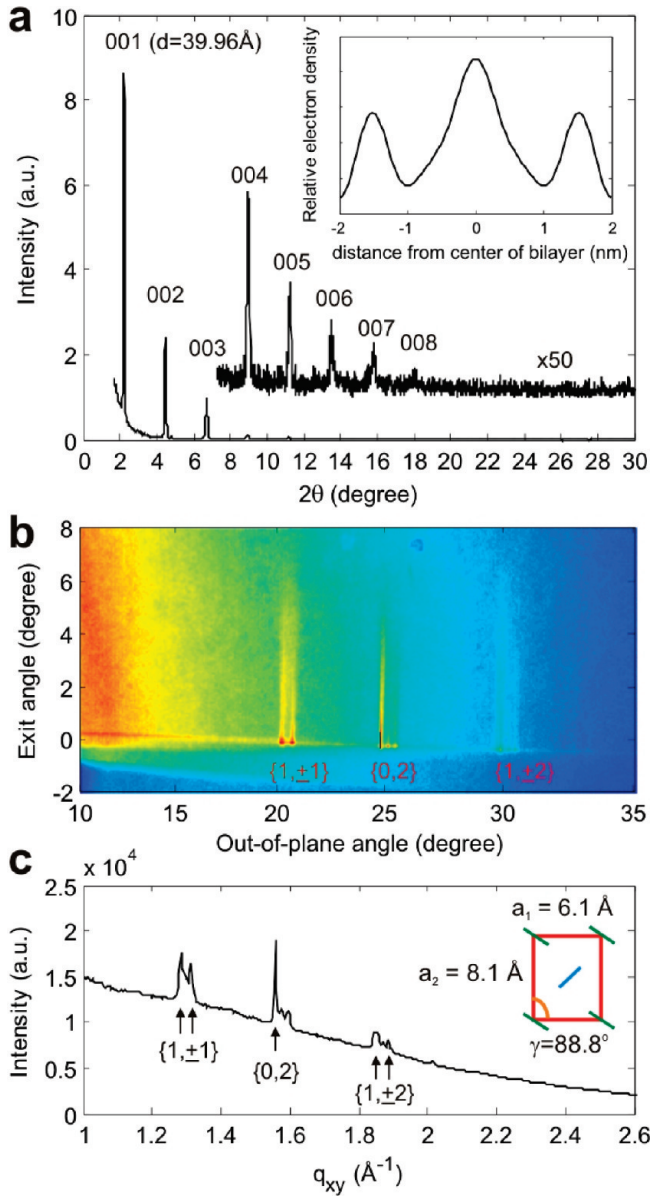

Figure 2. X-ray diffraction (XRD) and grazing-incidence X-ray diffraction (GIXD) of the nanolayers. (a) XRD shows multiple orders of diffraction peaks, indicating a well-ordered layered structure along the *z*-direction; the inset shows the relative electron density profile of the nanolayer reconstructed using (001)−(005) Bragg peak intensity. (b) GIXD with the indices marked for a distorted centered rectangular unit cell; (c) Linecut along the q_{xy} direction at $q_z \approx 0$. The inset shows the reduced in-plane lattice parameters.

higher concentration. It is also worthwhile to note that when just one active terminal is kept for the silane molecules, cross-linking between neighboring molecules is not possible, resulting in only monolayers.[4]

While AFM imaging captured the kinetic process of the layered growth on surfaces, we discovered the nanolayer configuration by a combination of infrared (IR) probing and quantum chemical (QC) modeling. Since IR peaks at 1027 and 1107 cm^{-1} are the signature of the antisymmetric stretching mode of siloxane (Si−O−Si),[34] we assigned polysiloxane as the inorganic portion of the layered stacking. After self-assembly, the lack of peaks at 910 cm^{-1} indicated depletion of silanol groups (Si−OH). QC modeling based on density functional theory (DFT) confirmed that the polysiloxane chain was the backbone of each individual layer. Along each single chain, as shown in Figure 4a, adjacent anthracyl moieties in the branches assumed an alternating up-and-down configuration due to the spatial confinement imposed by the linear siloxane unit for the anthracyl branches. When viewed from the perspective of an up-and-down configuration, the molecular layers are bilayer in nature. Due to a severe steric hindrance between anthracyl groups, the QC modeling also ruled out another alternative mode for bilayer-by-bilayer stacking, where organic portions are composed of interdigitated aromatic branches between neighboring layers.

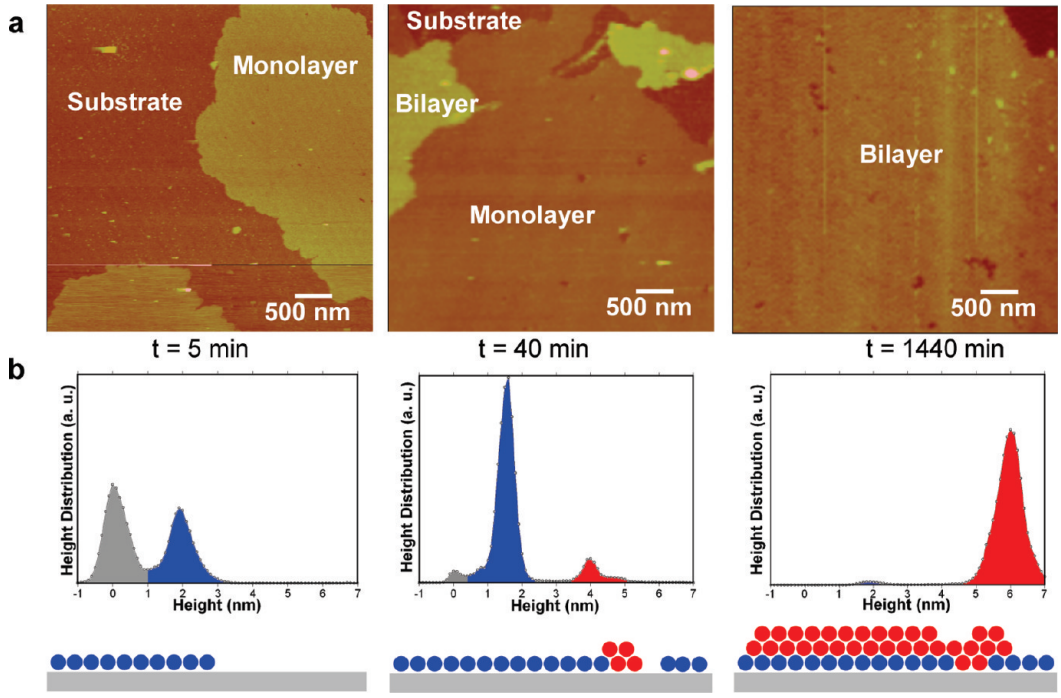

Figure 3. Self-assembly kinetics of ANS1 on a silicon wafer revealed by AFM: (Row a) AFM images of the sample at three stages of self-assembly; (row b) the corresponding height distribution of the AFM measurements, and the cartoons of the formation of the layers, where gray, blue, and red color designate the substrate, the monolayer, and the bilayer, respectively. (5−10 min) ANS1 starts to form a monolayer, the height being 2.4 nm. (40 min) The monolayer has grown into a larger, continuous film that covers almost all of the substrate. The patches of bilayers (4.3 nm in height) are atop the monolayer. (1440 min) The bilayer patches have grown into a continuous film, and the monolayer can no longer be seen. The pinhole of 2.4 nm in depth signals a monolayer underneath.

The more than 90° of contact angle over the surface of the nanolayers suggested a hydrophobic surface, with inorganic portions buried instead. More interestingly, configuration of the unit cells suggested that the aromatic branches interacted via $\pi-\pi$ stacking along the *y*-axis, with 3.1 Å distance in between and herringbone or T-stacking between the aromatic branches along the $x = y$ and $x = -y$ directions (Figure 4b). This motif produced a bilayer 4.3 nm in height, closely matching the AFM and XRD measurements. The nanolayers observed were explained when multiple bilayers were stacked vertically as shown in Figure 4c.

Organosilane has been known for its layered but amorphous construction during self-assembly.[26−28] Yet, the main contributor to those layers was from a continuous 2D network of $(SiO-O-SiO)_n$ rather than a simple 1D connection ($(Si-O-Si)_n$). Our 1D backbone of a linear polysiloxane allowed the branches to take on a close packing. Instead of letting ANS1 play an active role during self-assembly, one might think that grouping linear siloxane polymers directly could also produce a nanolayer-like crystal, but we found this not to be the case. When a linear polymer of ANS1 was obtained and a dilute solution of the polymer was carefully drop cast, a thin film was revealed with wormlike, coexisting multiple phases. This morphology and irregular packing suggested difficulty in aligning polymer chains directly into ordered 2D objects. This contrast motivated us to make the following hypothesis regarding the role of ANS1 in the formation of highly ordered nanolayers: the conjugated heads interacted through a combination of solvophobic interactions and $\pi-\pi$ cooperation to pre-form well-organized nuclei with the up-and-down configuration.[34−36] The solvophobic interaction contributes to the minimized exposure of polar tails to solvents by stacking the aromatic heads toward the outer surfaces of nuclei; the $\pi-\pi$ cooperation, on the other hand, gives the aromatic rings a dense and compact stacking in 2D. A subsequent condensation then completes the construction. Simply, ANS1 functions as a building block, where both solvophobic interactions and $\pi-\pi$ cooperation are the dual driving forces for the self-assembly.

To support this hypothesis, we first used octodecyldiethoxysilane, an alkylsilane with 18-carbon chains, as a control. Self-assembly resulted in a liquid substance, and further condensation revealed a gel-like material. We noted that the estimated stacking energy for the nanolayer of ANS1 was −2.4 kcal/mol per aromatic branch. When the anthracyl moieties were replaced by the octodecyl units, a much smaller stacking energy of −0.6 kcal/mol per octadecyl branch resulted. The general conclusion was that $\pi-\pi$ binding between anthracyl moieties contributed largely to the lamellar structure.

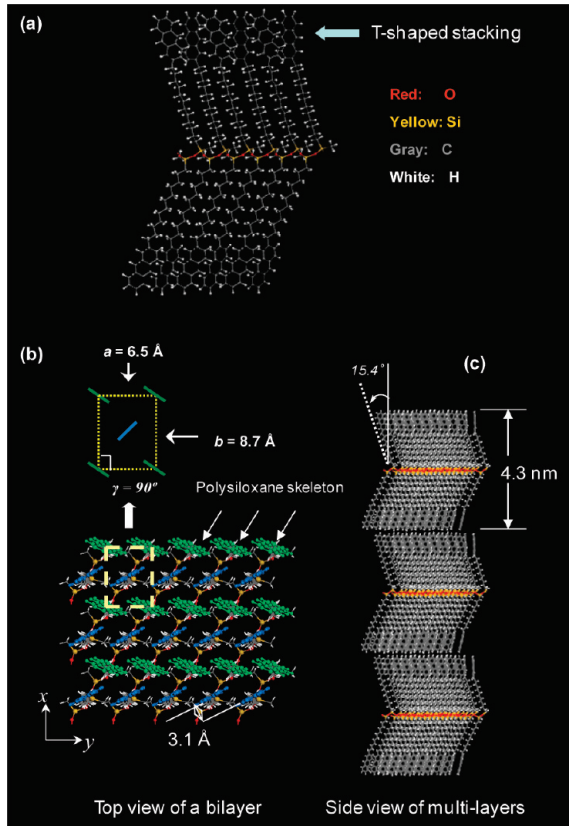

Figure 4. Theoretical model of the nanolayers. (a) Snapshot of a single polysiloxane chain, showing up-and-down orientation of anthracyl rings and the herringbone packing. (b) Packing motif of anthracyl rings and polysiloxane skeleton in the *x*−*y* plane. Only the upper part of a single layer is shown for simplicity. The packing motif suggests a coexisting π−π and herringbone packing along the *y* axis and polysiloxane chain, respectively. (c) Side view of layered stacking with the alignment of polysiloxane chains in two-dimensions.

The importance of the π−π interaction also manifested itself in two other systems closely related to ANS1: ANS2 ((4-(anthracen-2-yl)butyl)diethoxy(methyl)silane) and ANS3 ((4-(anthracen-9-yl)butyl)-diethoxy(methyl)-silane), both shown in Scheme 1. The assembled features from ANS2 were 2D-like, whereas the assembled features of ANS3 were amorphous nanoparticles. Clearly, a shorter alkyl chain reduced the intermolecular interactions by rendering a much rougher surface packing, whereas sufficiently discouraged π−π interaction disrupts the formation of an organized structure. Further, when such a π−π interaction did exist, a strong π−π coupling between aromatic branches produced a significant red-shift and peak widening in the UV−vis spectrum of the nanolayers.

Finally, when thin films were cast by using anthracene derivatives without silane terminals, they were found to be forming coexisting and porous monolayer-by-monolayer and monolayer-in-monolayer (or interdigitated) structures (see Supporting Information). In contrast to the aforementioned solid bilayer-by-bilayer structures, the dominance of a porous monolayer as the stacking unit suggests the importance of having a siloxane chain as the backbone of the nanolayer. Nevertheless, the appearance of a layered structure confirms the significant role of conjugated rings in the self-assembly process.

In summary, to pack conjugated molecules into a highly ordered and freestanding 2D structure, π-stitched silane can be used as a good building block as long as a linear polysiloxane chain is formed after polycondensation. The noncovalent π−π binding between conjugated moieties, as well as solvophobic interactions, will render a planar construction of nanolayers. The large, smooth, and structurally well-defined nanolayers will be a hybrid comprising alternating inorganic siloxane and organic conjugated moieties, which can be viewed as alternating insulation layers and organic semiconductor layers. Thanks to the tremendous progress in synthetic chemistry, chemical modification of the aromatic head and alkyl chain can lead to architectures with rich optoelectronic functions, and the highly ordered nanolayers formed are projected to find their way into organic electronics, piezoelectronics, nanoelectronics, and perhaps even energy storage.

METHODS

Synthesis of Anthracene-2-carboxylic Acid.[37] 9,10-dioxo-9,10-dihydroanthracene-2-carboxylic acid (0.0198 mol, 5.0 g), zinc (0.436 mol, 28.5 g) and NH_4OH (350 mL) were mixed and refluxed for 10 h. The reaction mixture was cooled to room temp (r.t.) and neutralized with aqueous HCl (6 M). The residue was filtered, and the paste atop was washed twice with water, generating the desired product as a light-yellow solid (4.23 g, 96%). The raw product was used as formed. Mp: 283−285 °C. ^{1}H NMR (300 MHz, DMSO-d_6): δ 8.73 (2H, s), 8.60 (1H, s), 8.12−8.04 (4H, m), 7.56 (2H, m). ^{13}C NMR (75 MHz, DMSO-d_6): 132.0, 131.9, 131.3, 130.6, 130.3, 128.2, 128.1, 127.4, 127.5, 126.1, 126.0, 125.8, 125,7. IR (neat): 1694. HREI: calcd for ($C_{15}H_{10}O_2$), 222.0681; found, 222.0685.

Synthesis of Anthracen-2-ylmethanol. Anthracene-2-carboxylic acid (4.4 g, 0.0198 mol) was dissolved in THF (200 mL) at 0 °C. BH_3-THF (1 M, 34 mL) was added slowly over 1 h, generating a turbid mixture. The reaction was kept at 0 °C for another hour, and then the temperature was slowly elevated to 50 °C and maintained at 50 °C for 40 h. Saturated sodium carbonate (200 mL) was added slowly to the cooled reaction, and the mixture was stirred for another hour. The top THF layer was removed, and the bottom aqueous layer was extracted with THF twice. The THF portions were combined and dried with magnesium sulfate. Removal of the THF resulted in anthracen-2-ylmethanol (3.62 g, 88%). Mp: 216−218 °C. ^{1}H NMR (300 MHz, THF-d_8): δ 8.41 (2H, s), 8.00−7.95 (4H, m), 7.46−7.40 (3H, m), 5.76 (2H, d, J = 5.4 Hz), 4.33 (1H, t, J = 5.7 Hz). ^{13}C NMR (75 MHz, THF-d_8): 139.0, 131.0, 130.9, 130.7, 130.3, 127.0, 126.9, 126.8, 124.8, 124.6, 124.0,1, 123.96, 123.8, 122.9, 63.14. HREI: calcd for ($C_{15}H_{12}O$), 208.0888; found, 208.0890.

Synthesis of 2-(Chloromethyl)anthracene.[38] To a solution of anthracen-2-ylmethanol (0.10 g, 0.45 mmol), DMAP (6 mg, 0.045 mmol), and triethylamine (55 mg, 0.54 mmol) in DCM (100 mL) under nitrogen at 0 °C was added dropwise methanesulfonyl chloride (57 mg, 0.50 mmol) over 5 min. After a further 2 h stirring at 0 °C, the mixture was warmed to r.t. and stirred overnight. The reaction mixture was washed with aqueous HCl (0.5 M),

and the aqueous phase was then extracted with DCM. The combined organic phases were washed with saturated aqueous potassium hydrogen carbonate solution, dried over magnesium sulfate, filtered, and evaporated to dryness, producing a light-yellow solid. Chromatographic purification of the solid with silica gel yielded the title compound (83 mg, 60%), and the R_f was 0.24 with hexane being the eluting solvent. Mp: 179−180 °C. ^{1}H NMR (400 MHz, $CDCl_3$): δ 8.44 (2H, d, J = 3.6 Hz), 8.06−8.00 (4H, m), 7.52−7.50 (3H, m), 4.82 (2H, s). ^{13}C NMR (100 MHz, $CDCl_3$): 134.1, 132.1, 132.0, 131.1, 129.2, 128.21, 121.18, 127.6, 126.6, 126.2, 125.72, 125.68, 47.0; HREI: calcd for ($C_{15}H_{11}Cl$), 226.0549; found, 226.0557.

Synthesis of 2-(Dodec-11-enyl)anthracene. 11-Bromoundec-1-ene (0.344 g, 1.48 mmol) and magnesium (0.071 g, 3 mmol) were mixed in THF (5 mL) and stirred at r.t. for 2 h to obtain a Grignard reagent. 2-(Chloromethyl)anthracene (0.20 g, 0.74 mmol) was dissolved in THF (10 mL). At r.t., the flask was purged with N_2 for 5 min, and then the above Grignard reagent was added over 10 min. After that, the reaction was stirred at r.t. for 2 h. Saturated aqueous NH_4Cl was added to quench the reaction. THF was removed, and CH_2Cl_2 was added to extract the aqueous leftover. CH_2Cl_2 portions were combined, dried with sodium sulfate, and removed, generating a light-yellow solid. Chromatographic purification of the solid with silica gel gave the title compound (0.158 g, 62%), and the R_f is 0.28 with hexane being the eluting solvent. The title compound contains a very small amount of 2-methylanthracene, which is extremely hard to remove. Mp: 77−80 °C (dec.). ^{1}H NMR (300 MHz, $CDCl_3$): δ 8.39−8.35 (2H, m), 8.01−7.93 (3H, m), 7.76 (1H, s), 7.46−7.43 (2H, m), 7.36−7.32 (1H, dd, J = 1.55 and 8.60 Hz), 5.89−5.75 (1H, m), 5.04−4.91 (2H, m), 2.81 (2H, t, J = 7.32 Hz), 2.04 (2H, q, J = 7.32 Hz), 1.75 (2H, p, J = 6.80 Hz), 1.45−1.17 (14H, m). ^{13}C NMR (75 MHz, $CDCl_3$): 140.1, 139.5, 132.2, 132.0, 131.4, 130.8, 128.4, 128.3, 128.2, 127.8, 126.1, 126.0, 125.6, 125.4, 125.1, 114.3, 36.5, 34.0, 31.2, 29.9, 29.81, 29.77, 29.7, 29.6, 29.4, 29.2. HREI: calcd for ($C_{26}H_{32}$), 344.2504; found, 344.2510.

Synthesis of (12-(Anthracen-2-yl)dodecyl)diethoxy(methyl)silane.[39] In a pressure tube, 2-(dodec-11-enyl)anthracene (0.15 g, 0.43 mmole) and diethoxy(methyl)silane 1(0.41 g, 3.1 mmol) were mixed, stirred, and purged with N_2 for 5 min. PtO_2 (6 mg, 0.035 mmol) was poured into the tube, and the tube was sealed immediately. The reaction was heated at 80 °C for 18 h and then cooled down, and the excessive liquids were removed under vacuum. Chromatographic purification of the residue with silica gel resulted in the title compound (98 mg, 48%), and the R_f was 0.41 with the eluting solvent being a mixture of ethyl acetate and hexane (v/v 5:95). Mp: 64−68 °C (dec.). ^{1}H NMR (400 MHz, $CDCl_3$), δ 8.41 (1H, S), 8.36 (1H, s), 8.02−7.94 (3H, m), 7.77 (1H, s), 7.47−7.45 (2H, m), 7.36 (1H, d, J = 8.7 Hz), 3.78 (4H, q, J = 7.0 Hz), 2.82 (2H, t, J = 8.1 Hz), 1.76 (2H, p, J = 8.1 Hz), 1.42−1.22 (24H, m), 0.65−0.62 (2H, m), 0.13 (3H, s). ^{13}C NMR (100 MHz, $CDCl_3$): 139,9, 132.0, 131.9, 131.3, 130.6, 128.2, 128.04, 127,99, 127.6, 125.9, 125.8, 125.3, 125.2, 124.9, 58.0, 36.31, 33.3, 31.0, 29.7, 29.62, 29.57, 29.4, 29.3, 22.9, 18.4, 13.8, −4.86. HREI: calcd for ($C_{31}H_{46}O_2Si$), 478.3267; found, 478.3265. A side product, 2-*n*-dodecylanthracene, was also obtained. ^{1}H NMR (400 MHz, $CDCl_3$): δ 8.36 (1H, s), 8.32 (1H, s), 7.96 (2H, m), 7.91 (1H, d, J = 8.8 Hz), 7.73 (1H, s), 7.41 (2H, m), 7.31 (1H, dd, J = 8.7 and 1.5 Hz), 2.78 (2H, t, J = 7.8 Hz), 1.72 (2H, m), 1.44−1.12 (18H, m), 0.85 (3H, t, 7.0 Hz). HRFAB: calcd ($C_{26}H_{34}$), 346.2661; found, 346.2662.

Synthesis of 2-(But-3-enyl)anthracene. 2-(Chloromethyl)anthracene and allylmagnesium chloride (2 M in THF) were used to synthesize this compound (yield, 60%), following a procedure similar to that used for 2-(dodec-11-enyl)anthracene. Mp: 133−135 °C. ^{1}H NMR (400 MHz, $CDCl_3$): δ 8.37 (1H, s), 8.33 (1H, s), 7.97 (2H, m), 7.92 (1H, d, J = 8.6 Hz),7.75 (1H, s), 7.42 (2H, m), 7.32 (1H, dd, J = 8.8 and 1.7 Hz), 5.91 (1H, m), 5.07 (1H, dq, J = 17.2 and 1.8 Hz), 4.99 (1H, dm, 10.3 Hz), 2.89 (2H, t, J = 8.2 Hz), 2.49 (2H, m). ^{13}C NMR (75 MHz, $CDCl_3$): δ138.76, 138.03, 131.90, 131.82, 131.31, 130.57, 128.17, 128.12, 128.06, 127.42, 125.97, 125.94, 125.45, 125.26, 124.99, 115.11, 35.71, 35.06. HREI: calcd for ($C_{18}H_{16}$), 232.1252; found, 232.1262.

Synthesis of (4-(Anthracen-2-yl)butyl)diethoxy(methyl)silane. 2-(But-3-enyl)anthracene and diethoxy(methyl)silane were used to synthesize the yellow title compound (yield, 40%), following a procedure similar to that used for (12-(anthracen-2-yl)dodecyl)diethoxy(methyl)silane. Mp: ~140 °C (dec). ^{1}H NMR (400 MHz, $CDCl_3$): δ 8.36 (1H, s), 8.32 (1H, s), 7.97 (2H, m), 7.92 (1H, d, J = 8.8 Hz), 7.73 (1H, s), 7.42 (2H, m), 7.32 (1H, dd, J = 8.6 and 1.5 Hz), 3.76 (4H, q, 5.2 Hz), 2.81 (2H, t, J = 7.5 Hz), 1.79 (2H, p, 7.7 Hz), 1.50 (2H, m), 1.20 (6H, t, J = 6.9 Hz), 0.71 (2H, m), 0.11 (3H, s). ^{13}C NMR (75 MHz, $CDCl_3$): δ 139.64, 132.01, 131.84, 131.28, 130.59, 128.18, 128.06, 128.04, 127.55, 125.90, 125.79, 125.36, 125.20, 124.91, 58.10, 35.95, 34.50, 22.67, 18.43, 13.79, −4.81. HREI: calcd for ($C_{23}H_{30}O_2Si$), 366.2015; found, 366.2033. A side product, 2-*n*-butylanthracene was also separated. ^{1}H NMR (400 MHz, $CDCl_3$): δ 8.36 (1H, s), 8.32 (1H, s), 7.96 (2H, m), 7.91 (1H, d, J = 8.7 Hz),7.73 (1H, s), 7.42 (2H, m), 7.32 (1H, dd, J = 8.7 and 1.6 Hz), 2.79 (2H, t, J = 7.8 Hz), 1.72 (2H, m), 1.41 (2H, m) 0.95 (3H, t, 7.3 Hz). HRFAB: calcd ($C_{18}H_{18}$), 234.1409; found, 234.1411.

Synthesis of 9-(Bromomethyl)anthracene. A mixture of PPh_3 (5.61 g, 21.4 mmol) in 40 mL of anhydrous acetonitrile was flushed with argon for 20 min, then bromine (3.42 g, 21.4 mmol) was added dropwise to the stirring solution. The mixture was continuously flushed with argon and 9-methanolanthracene (4.55 g, 21.8 mmol) in acetonitrile (10 mL) was then poured in quickly. The reaction was stirred for 1 h before being refrigerated overnight (5 °C). After it cooled to −5 °C for 30 min, the mixtue was filtered; and the solid on top was washed with cold acetonitrile (15 mL, 5 °C). This procedure generated the yellow title compound in high quality and in good yield (96%). ^{1}H NMR (400 MHz, $CDCl_3$): δ 8.48 (1H, s), 8.29 (2H, dq, J = 8.9 and 0.7 Hz), 8.02 (2H, dm, J = 8.5 Hz), 7.63 (2H, tm, J = 6.6 Hz), 7.49 (2H, tm, J = 6.6 Hz), 5.53 (2H, s) .^{13}C NMR (75 MHz, $CDCl_3$): δ 131.60, 129.73, 129.27, 129.18, 127.87, 126.79, 125.37, 123.51, 26.94.

Synthesis of 9-(But-3-enyl)anthracene. 9-(Bromomethyl)anthracene and allylmagnesium chloride (2 M in THF) were used to synthesize this compound (yield, 62%), following a procedure similar to that used for 2-(dodec-11-enyl)anthracene. Mp: 59−61 °C. ^{1}H NMR (400 MHz, $CDCl_3$): δ 8.34 (1H, s), 8.25 (2H, d, J = 8.6 Hz), 8.00 (2H, d, J = 8.2 Hz), 7.48 (4H, m), 6.05 (1H, m), 5.20 (1H, dq, J = 15.53 and 1.7 Hz), 5.07 (1H, dm, J = 10.2 Hz), 3.70 (2H, m), 2.55(2H, m). ^{13}C NMR (75 MHz, $CDCl_3$): δ 138.29, 134.23, 131.63, 129.55, 129.25, 125.82, 125.54, 124.85, 124.37, 114.98, 35.15, 27.43. HREI: calcd for ($C_{18}H_{26}$), 232.1252; found, 232.1252.

Synthesis of (4-(Anthracen-9-yl)butyl)diethoxy(methyl)silane. 9-(But-3-enyl)anthracene and diethoxy(methyl)silane were used to synthesize this yellow liquid compound (yield, 42%), following a procedure similar to that used for (12-(anthracen-2-yl)dodecyl)diethoxy(methyl)silane. ^{1}H NMR (400 MHz, $CDCl_3$): δ 8.31 (1H, s), 8.24 (2H, d, J = 8.7 Hz), 7.98 (2H, d, J = 8.4 Hz), 7.45 (4H, m), 3.76 (4H, q, J = 6.8 Hz), 3.58 (2H, m), 1.83 (2H, m), 1.67 (2H, m), 1.21 (6H, t, J = 7.1 Hz), 0.75 (2H, m), 0.13 (3H, s). ^{13}C NMR (75 MHz, $CDCl_3$): δ 135.27, 131.63, 129.49, 129.18, 125.47, 125.33, 124.78, 124.47, 58.15, 34.84, 27.83, 23.72, 18.44, 13.88, −4.84. HREI: calcd for ($C_{23}H_{30}O_2Si$), 366.2015; found, 366.2025.

Nanolayer Growth. The substrates were pretreated in advance according to the literature. The silicon wafer was sonicated in acetone for 10 min followed by another 10 min in ethanol and then immersed in a mixture of concentrated H_2SO_4 and 30% H_2O_2 (v/v 1:1) for 20 min. This pretreated silicon wafer was then blown dry with N_2 and stored under N_2 for future use. During film casting, the wafer was either immersed in an ANS1 solution (10^{-4} M in THF, with trace amount of water) for 24 h or placed over a countertop to receive ANS1 droplets before drying in an ambient environment. It was then copiously rinsed with ethanol and baked at 80 °C for 1 h. All of the thin film samples were stored under a N_2 environment for future use.

Acknowledgment. The authors thank Professor Patrick H. Dussault and his group members, as well as Mr. Alexandre Dhôtel, for their generous help and gratefully acknowledge the partial financial support from the National Science Foundation (CMMI 0825905 and CMMI 0900644) and the Army Research Office (W911NF-08-1-0190; Program Manager: Dr. Dwight Woolard).

Supporting Information Available: A description of the experimental procedures and computational details. This material is available free of charge *via* the Internet at http://pubs.acs.org.

REFERENCES AND NOTES

1. Yan, Q.; Huang, B.; Yu, J.; Zheng, F.; Zang, J.; Wu, J.; Gu, B. L.; Liu, F.; Duan, W. Intrinsic Current-Voltage Characteristics of Graphene Nanoribbon Transistors and Effect of Edge Doping. *Nano Lett.* **2007**, *7*, 1469–1473.
2. Gandhi, D. D.; Lane, M.; Zhou, Y.; Singh, A. P.; Nayak, S.; Tisch, U.; Eizenberg, M.; Ramanath, G. Annealing-Induced Interfacial Toughening Using a Molecular Nanolayer. *Nature* **2007**, *447*, 299–302.
3. Geim, A. K. Graphene: Status and Prospects. *Science* **2009**, *324*, 1530–1534.
4. Smits, E. C. P.; Mathijssen, S. G. J.; van Hal, P. A.; Setayesh, S.; Geuns, T. C. T.; Mutsaers, K. A. H. A.; Cantatore, E.; Wondergem, H. J.; Werzer, O.; Resel, R.; *et al*. Bottom-Up Organic Integrated Circuits. *Nature* **2008**, *455*, 956–959.
5. Yang, L.; Peng, H; Huang, K; Mague, J. T.; Li, H.; Lu, Y. Hierarchical Assembly of Organic/Inorganic Building Molecules with π−π Interactions. *Adv. Funct. Mater.* **2008**, *18*, 1526–1535.
6. Diegelmann, S. R.; Gorham, J. M.; Tovar, J. D. One-Dimensional Optoelectronic Nanostructures Derived from the Aqueous Self-Assembly of π-Conjugated Oligopeptides. *J. Am. Chem. Soc.* **2008**, *130*, 13840–13841.
7. Calhoun, M. F.; Sanchez, J.; Olaya, D.; Gershenson, M. E.; Podzorov, V. Electronic Functionalization of the Surface of Organic Semiconductors with Self-Assembled Monolayers. *Nat. Mater.* **2008**, *7*, 84–89.
8. Feng, D. Q.; Wisbey, D.; Tai, Y.; Losovyj Ya, B.; Zharnikov, M.; Dowben, P. A. Abnormal Temperature Dependence of Photoemission Intensity Mediated by Thermally Driven Reorientation of a Monomolecular Film. *J. Phys. Chem. B* **2006**, *110*, 1095–1098.
9. Halik, M.; Klauk, H.; Zschieschang, U.; Schmid, G.; Dehm, C.; Schutz, M.; Maisch, S.; Effenberger, F.; Brunnbauer, M.; Stellacci, F. Low-Voltage Organic Transistors with an Amorphous Molecular Gate Dielectric. *Nature* **2004**, *431*, 963–966.
10. Sayyad, M. H.; Saleem, M.; Karimov, K. S.; Yaseen, M.; Ali, M.; Cheong, K. Y.; Noor, A. F. M. Synthesis of Zn(II) 5,10,15,20-Tetrakis(4′-isopropylphenyl) Porphyrin and Its Use as a Thin Film Sensor. *Appl. Phys. A: Mater. Sci. Process.* **2010**, *98*, 103–109.
11. Nuzzo, R. G.; Allara, D. L. Adsorption of Bifunctional Organic Disulfides on Gold Surfaces. *J. Am. Chem. Soc.* **1983**, *105*, 4481–4483.
12. Xu, S.; Cruchon-Dupeyrat, S. J. N.; Garno, J. C.; Liu, G. Y.; Jennings, G. K.; Yong, T. H.; Laibinis, P. E. *In Situ* Studies of Thiol Self-Assembly on Gold From Solution Using Atomic Force Microscopy. *J. Chem. Phys.* **1998**, *108*, 5002–5012.
13. Yu, J. J.; Tan, Y. H.; Li, X.; Kuo, P. K.; Liu, G. Y. A Nanoengineering Approach to Regulate the Lateral Heterogeneity of Self-Assembled Monolayers. *J. Am. Chem. Soc.* **2006**, *128*, 11574–11581.
14. Xu, S.; Laibinis, P. E.; Liu, G. Y. Accelerating the Kinetics of Thiol Self-Assembly on Gold—A Spatial Confinement Effect. *J. Am. Chem. Soc.* **1998**, *120*, 9356–9361.
15. Dhirani, A. A.; Zehner, R. W.; Hsung, R. P.; GuyotSionnest, P.; Sita, L. R. Self-Assembly of Conjugated Molecular Rods: A High-Resolution STM Study. *J. Am. Chem. Soc.* **1996**, *118*, 3319–3320.
16. Maya, F.; Flatt, A. K.; Stewart, M. P.; Shen, D. E.; Tour, J. M. Formation and Analysis of Self-Assembled Monolayers from U-Shaped Oligo(phenylene ethynylene)S as Candidates for Molecular Electronics. *Chem. Mater.* **2004**, *16*, 2987–2997.
17. Sabatani, E.; Cohenboulakia, J.; Bruening, M.; Rubinstein, I. Thioaromatic Monolayers On Gold—A New Family of Self-Assembling Monolayers. *Langmuir* **1993**, *9*, 2974–2981.
18. Ulman, A. Self-Assembled Monolayers of 4-Mercaptobiphenyls. *Acc. Chem. Res.* **2001**, *34*, 855–863.
19. Maoz, R.; Matlis, S.; DiMasi, E.; Ocko, B. M.; Sagiv, J. Self-Replicating Amphiphilic Monolayers. *Nature* **1996**, *384*, 150–153.
20. Tillman, N.; Ulman, A.; Elman, J. F. A Novel Self-Assembled Monolayer Film Containing a Sulfone-Substituted Aromatic Group. *Langmuir* **1990**, *6*, 1512–1518.
21. Ulman, A. Formation and Structure of Self-Assembled Monolayers. *Chem. Rev.* **1996**, *96*, 1533–1554.
22. Zang, L.; Che, Y. K.; Moore, J. S. One-Dimensional Self-Assembly of Planar π-Conjugated Molecules: Adaptable Building Blocks for Organic Nanodevices. *Acc. Chem. Res.* **2008**, *41*, 1596–1608.
23. Cui, H.; Muraoka, T.; Cheetham, A. G.; Stupp, S. I. Self-Assembly of Giant Peptide Nanobelts. *Nano Lett.* **2009**, *9*, 945–951.
24. Zubarev, E. R.; Pralle, M. U.; Sone, E. D.; Stupp, S. I. Self-assembly of Dendron Rodcoil Molecules into Nanoribbons. *J. Am. Chem. Soc.* **2001**, *123*, 4105–4106.
25. Shimojima, A.; Sugahara, Y.; Kuroda, K. Inorganic−Organic Layered Materials Derived *via* the Hydrolysis and Polycondensation of Trialkoxy(Alkyl)Silanes. *Bull. Chem. Soc. Jpn.* **1997**, *70*, 2847–2853.
26. Huo, Q. S.; Margolese, D. I.; Stucky, G. D. Surfactant Control of Phases in the Synthesis of Mesoporous Silica-Based Materials. *Chem. Mater.* **1996**, *8*, 1147–1160.
27. Parikh, A. N.; Schivley, M. A.; Koo, E.; Seshadri, K.; Aurentz, D.; Mueller, K.; Allara, D. L. *N*-Alkylsiloxanes: from Single Monolayers to Layered Crystals. The Formation of Crystalline Polymers from The Hydrolysis of *N*-Octadecyltrichlorosilane. *J. Am. Chem. Soc.* **1997**, *119*, 3135–3143.
28. Jiang, J.; Lima, O. V.; Pei, Y.; Zeng, X. C.; Tan, L.; Forsythe, E. Dipole-Induced, Thermally Stable Lamellar Structure by Polar Aromatic Silane. *J. Am. Chem. Soc.* **2009**, *131*, 900–901.
29. Dautel, O. J.; Robitzer, M.; Lere-Porte, J. P.; Serein-Spirau, F.; Moreau, J. J. E. Self-Organized Ureido Substituted Diacetylenic Organogel. Photopolymerization of One-Dimensional Supramolecular Assemblies To Give Conjugated Nanofibers. *J. Am. Chem. Soc.* **2006**, *128*, 16213–16223.
30. Luo, Y.; Lin, J.; Duan, H.; Zhang, J.; Lin, C. Self-Directed Assembly of Photoactive Perylenediimide-Bridged Silsesquioxane into a Superlong Tubular Structure. *Chem. Mater.* **2005**, *17*, 2234–2236.
31. van der Boom, M. E.; Evmenenko, G.; Yu, C.; Dutta, P.; Marks, T. J. Interrupted-Growth Studies of the Self-Assembly of Intrinsically Acentric Siloxane-Derived Monolayers. *Langmuir* **2003**, *19*, 10531–10537.
32. Onclin, S.; Ravoo, B. J.; Reinhoudt, D. N. Engineering Silicon Oxide Surfaces Using Self-Assembled Monolayers. *Angew. Chem., Int. Ed.* **2005**, *44*, 6282–6304.
33. Schwartz, D. K.; Steinberg, S.; Israelachvili, J.; Zasadzinski, J. A. N. Growth of a Self-Assembled Monolayer by Fractal Aggregation. *Phys. Rev. Lett.* **1992**, *69*, 3354–3357.
34. Kakudo, M.; Kasai, P. N.; Watase, T. Crystal Structure of Silanols and Their Infrared Spectra. *J. Chem. Phys.* **1953**, *21*, 1894–1895.
35. Zheng, H. ; Smith, R. K.; Jun, Y.-w.; Kisielowski, C.; Dahmen, U.; Alivisatos, A. P. Observation of Single Colloidal Platinum Nanocrystal Growth Trajectories. *Science.* **2009**, *324*, 1309–1312.
36. Zhou, Q.; Zhang, J.; Ren, Z.; Yan, S.; Xie, P.; Zhang, R. A Stable and High-Efficiency Blue-Light Emitting Terphenyl-Bridged Ladder Polysiloxane. *Macromol. Rapid Commun.* **2008**, *29*, 1259–1263.
37. Karatsu, T.; Arai, T.; Sakuragi, H.; Tokumaru, K.; Wirz, J. Semiempirical Calculation of the Triplet−Triplet Absorption Spectra of 2-Anthrylethylenes Undergoing Photochemical One-Way Isomerization. *Bull. Chem. Soc. Jpn.* **1994**, *67*, 891–894.
38. Aathimanikandan, S. V.; Sandanaraj, B. S.; Arges, C. G.; Bardeen, C. J.; Thayumanavan, S. Effect of Guest Molecule Flexibility in Access to Dendritic Interiors. *Org. Lett.* **2005**, *7*, 2809–2812.
39. Sabourault, N.; Mignani, G.; Wagner, A.; Mioskowski, C. Platinum Oxide (PtO_2): A Potent Hydrosilylation Catalyst. *Org. Lett.* **2002**, *4*, 2117–2119.